Article

Effect of Reinforcement Type and Dispersion on the Hardening of Sintered Pure Aluminium

Omid Emadinia [1,2,*] , **Maria T. Vieira** [3] and **Manuel F. Vieira** [1,2]

1   CEMMPRE, Department of Metallurgical and Materials Engineering, University of Porto,
    Rua Dr. Roberto Frias, 4200-465 Porto, Portugal; mvieira@fe.up.pt
2   INEGI-Institute of Science and Innovation in Mechanical and Industrial Engineering, Rua. Dr. Roberto Frias,
    4200-465 Porto, Portugal
3   CEMMPRE, Department of Mechanical Engineering, University of Coimbra, Rua Luís Reis Santos,
    3030-788 Coimbra, Portugal; teresa.vieira@dem.uc.pt
*   Correspondence: omid.emadinia@fe.up.pt; Tel.: +351-92-434-2143

Abstract: The homogeneity of dispersion and reinforcing of pure aluminium by multi-walled carbon nanotubes (MWCNT) through the application of a high speed sonication (340 Hz) assisted by ultrasonication (35 kHz) was evaluated, this method was termed "assisted sonication". Other reinforcements (graphene, nanoalumina, and ultrafine tungsten carbide) were used for comparison with the MWCNT. The hardness measurement enabled us to evaluate the strengthening effect of the reinforcements. Raman analysis was the technique selected to evaluate the integrity of MWCNTs during dispersion. The scanning and transmission electron microscopies revealed the dispersion and microstructure of the nanoreinforcements and nanocomposites. After applying the assisted sonication, the MWCNTs were detangled without exfoliation. The integrity of MWCNTs was strongly influenced by the presence of the aluminum powder during dispersion. The application of the assisted sonication method reduced the size of the aggregates in the matrix, in comparison with the sonication technique. Ultrafine tungsten carbide, with a 1 vol. %, was the reinforcement that more effectively hardened aluminum due to a good dispersion of the reinforcement, grain refinement and the formation of $Al_{12}W$ phase.

Keywords: Aluminum powder; nanocomposite; reinforcement; dispersion; electron microscopy; hardness

1. Introduction

Producing metal matrix nanocomposites (MMNCs) through powder metallurgy (PM) routes can involve dispersing the nanoreinforcement among metal powders, and this is generally followed by compaction and sintering. The homogeneity of nanoreinforcement dispersion in the matrix is the most commonly recognized problem, e.g., multi-walled carbon nanotubes (MWCNT) strongly agglomerate [1–3], and their importance increases with increasing nanoreinforcement content [4,5]. The agglomeration is due to Van der Waals forces [6] and [7] (pp. 199–255), i.e., attraction rather than dispersion. Nonetheless, the tendency to produce MMNCs is high, as they benefit from the exclusive properties of nanomaterials [7] (pp. 199–255). This being the case, some shortcomings of micro size reinforcements can be eliminated, e.g., weight gain and crack formation [8,9]. After replacing the micro reinforcements with the nanosized ones, higher mechanical properties were reported [1,10]. One study summarized the possible contributions of several mechanisms to the strengthening of metal matrices, namely Hall Petch, Load Transferring, Orowan, and Thermal/Modulus Mismatch effects [11].

This study used the pure aluminum (Al), which is a light metal with a high workability [12] (p. 7), widely used, and recycled. The Al is used as an alloy and composite in automotive and aeronautic structural applications [13,14]. For pure Al no ageing is needed, and the strengthening mechanism is attained in the absence of any phase formation that could have been caused by the alloying elements. Nanoreinforcements are normally nanoceramic particulates, intermetallic compounds or carbon allotropes [1,15] (pp. 185–207) and [11] directly added to the matrix, or produced through in situ reactions during processing, e.g., mechanical alloying [11,16]. This study used the MWCNT, graphene nanosheets, nanoalumina, and ultrafine tungsten carbide (WC) reinforcements. These reinforcements are different in terms of surface area, size distribution, shape factor, and structure (4S) and density, and different interactions with the Al matrix are expected. A related study reported high dispersion efficiency of the MWCNTs with large diameters, over the thin nanotubes, and the strengthening of an Al matrix [17]. The MWCNT and graphene have densities close to that of the Al, while the nanoalumina and WC have slight and considerable differences, respectively. The nanoalumina particles agglomerate due to the Van der Waals forces; the MWCNTs are also tangled due to the tubular and flexible structure.

Mixing the composite constituents through PM approach can involve different techniques such as mechanical stirring (like ball milling), physical dispersing (like sonication), or a polymer assisted dispersion [18–23]. Occasionally a solution treatment such as functionalization is used to increase the surface properties of the carbon nanoparticles and improve the dispersion [3,6].

The feasibility of strengthening a pure Al powder (with maximum particle size of 22 μm) by dispersing 0.75 wt. % MWCNTs in the matrix by means of a high speed dispersing technique (sonication) has already been confirmed (~47% increase for hardness) [24], although this was strongly affected by the dispersing time [25]. Using an ultrasonication bath is a well-known mixing technique used for producing polymeric matrix composites [26,27] and graphene nanosheets [28], thus the assistance of this technique could also improve the dispersion. Some authors [29] presented the same hardening tendency for Al and Ni powders, with similar size distributions, dispersed by the same technique and with volume fractions of MWCNT up to 2%.

This study aimed to evaluate the hardening of a pure Al, with different 4S in respect to the previous study [24], by microhardness measurement. This research started by Al-MWCNT mixtures dispersed through a probe-like sonication technique (hereinafter referred to simply as sonication) and then it was assisted by an ultrasonication bath for MWCNT. The processing conditions led to the best hardening of Al-MWCNT composite were selected for the preparation of the Al with graphene nanosheets, nanoalumina, and ultrafine WC particles. Since the ultrasonication is a technique used for producing graphene nanosheets by exfoliating graphite particles [28], it can be chosen to disentangle pristine graphene sheets with the least damage. For this study the nanocomposite constituents were evaluated by scanning electron microscopy (SEM), assisted by secondary electrons (SE) and backscattered electrons (BSE) modes, and transmission electron microscopy (TEM). Raman spectroscopy was used to evaluate the influence of processing conditions on carbon nanotubes [30]. The microhardness measurement was considered as a criterion for evaluation of the reinforcing effect after sintering. The electron backscattered diffraction (EBSD) was used for characterizing the reinforced specimens.

2. Materials and Methods

The Al powder was supplied by Alfa Aesar with a purity of 99.8 wt. % and with 0.1 wt. % Fe as the major impurity. The chemical composition was determined by a PANalytical X-ray Fluorescence spectrometer (PANalytical AXIOSmax, PANalytical B.V., Almelo, The Netherlands). This powder has a density of 2670 kg/m^3, measured by a Helium pycnometer (micromeritics AccuPyc 1330, Micromeritics Instrument Corporation, Norcross, GA, USA). The Al powder characteristics such as powder morphology and particle size distribution (PSD) are presented in Figure 1a and Table 1, analyzed by SEM (FEI-Quanta 400 FEG equipment, FEI Company, Hillsboro, OR, USA), and a Malvern Laser scattering diffraction instrument (Mastersizer 3000, Malvern Instruments Limited,

Worcestershire, UK), respectively. Pristine MWCNT was supplied by FIBERMAX composites, which are in large agglomerates (Figure 1b) and have an average external diameter of 23 ± 7 nm (measured by ImageJ, 1.51r, Wayne Rasband, National Institutes of Health, Bethesda, MD, USA). These nanotubes have a density of 2013 kg/m^3. Graphene nanosheets (multilayer flakes with 98.5% purity) were supplied by Graphene Supermarket (Figure 1c), the WC (99.8% purity) by H.C. Starck Tungsten GmbH (Table 1 and Figure 1d), and the nanoalumina by Sigma Aldrich (Table 1). The TEM (FEI TECNAI G2 20 S-TWIN, FEI Company, Hillsboro, OR, USA) was used to observe the nanoreinforcements.
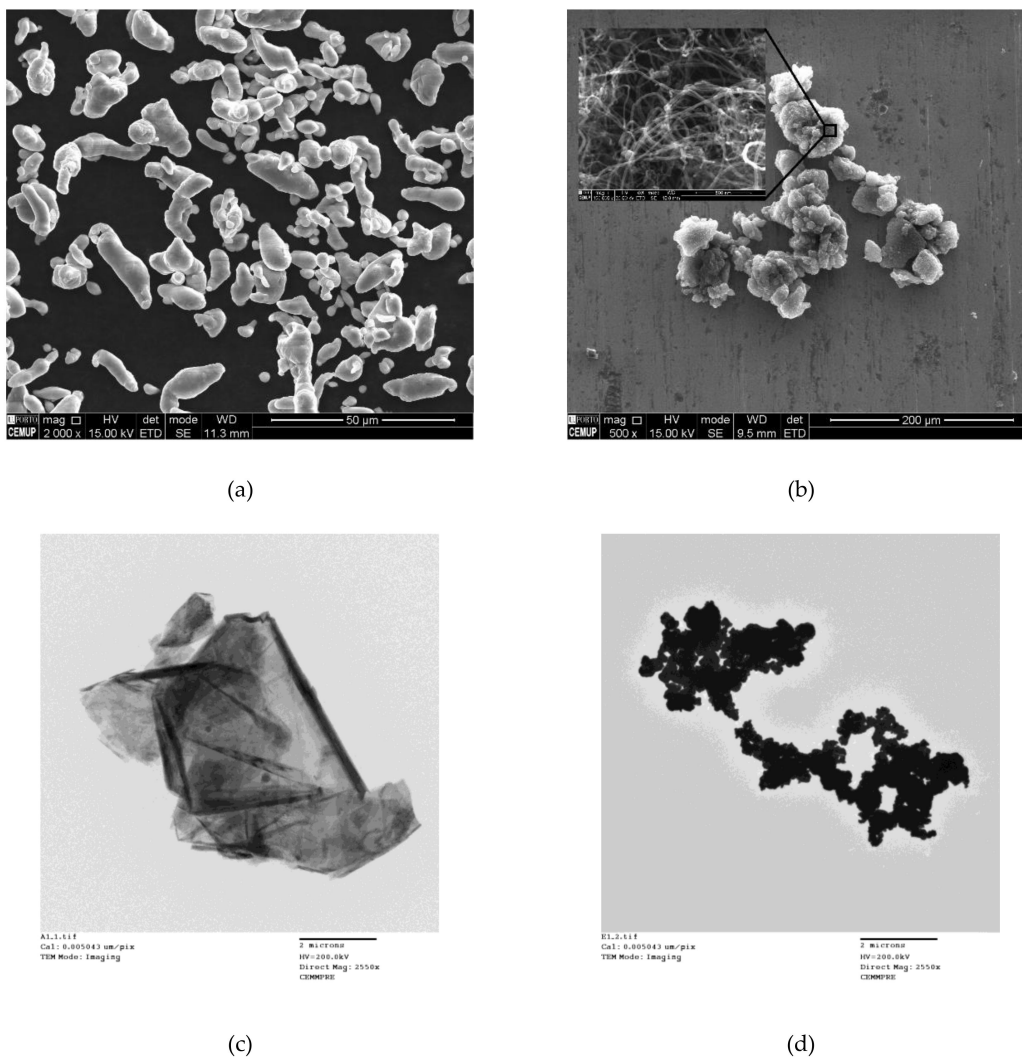

(a)

(b)

(c)

(d)

Figure 1. Scanning electron microscopy, secondary electrons mode (SEM/SE) images from (**a**) the Al powder and (**b**) from the pristine multi-walled carbon nanotubes (MWCNT); Transmission electron microscopy (TEM) images from the (**c**) pristine Graphene and (**d**) tungsten carbide (WC).

Table 1. Particle characteristics of some constituents.

Material	Particle size	Surface area (m^2/kg)	Density (kg/m^3)
Al	$D_{50} = 10.10$ μm	695	2670
Graphene	Average thickness 60 nm [1] Lateral size ≤ 7 μm [1]	$\leq 40{,}000$ [1]	2200 [2]
Al$_2$O$_3$	Particle size < 50 nm [1]	>40,000 [1]	3955 [2]
WC	$D_{50} = 0.33$ μm	19,000	15,630 [2]

[1] Supplier web page; [2] Theoretical values.

Dispersion of the preliminary Al-MWCNT nanocomposite, in isopropanol, involved four techniques: (1) Sonication (IKA T 25 Digital), this instrument can produce a wide range of 3000 to 25,000 rpm in 1–2 L of water and is assembled with a S 25 D-14 G-KS dispersing plastic blade; (2) magnetic stirring (1000 rpm for 5 h); (3) blending by a Turbula Shaker; and (4) an ultrasonication bath with 35 kHz power. Next, the powder-dispersants were filtered and dried in an oven at 80 °C for 60 min; the mixtures were compacted, at room temperature, under uniaxial stress into disks with 10 mm diameter and a thickness of almost 2 mm. Three uniaxial stresses were applied: 152, 300 and 400 MPa. The preparation was accomplished by sintering in a high vacuum ($\sim 5 \times 10^4$ Pa) at 640 °C for 120 min in a horizontal electric furnace. Microhardness measurements were performed by Struers Duramin equipment (Struers A/S, Ballerup, Denmark), using a 98 mN load (HV 10 gf in ASTM E384-1999), ten tests were performed on cross-sections of each sample. All microhardness measurements are accompanied by standard deviation (SD) values. The densities of sintered specimens were measured by the Archimedes technique (the scale was a METTLER TOLEDO AB204-S with 1 mg error). Three samples for each condition were tested and the densification is reported as the fraction of the measured density over the theoretical density.

The preliminary nanocomposite preparation involved sonicating the Al and MWCNTs (with 0, 0.25, 0.5, 0.75, 1.0 and 2.0 wt. % MWCNT), simultaneously, at 20,400 rpm for 15 min in isopropanol (~0.02 g/mL solid concentration) at room temperature, in line with the related study [24]. The microhardness measurements were considered as the criterion for evaluating the sintered specimens. These dispersion conditions were altered to maximize the reinforcement effect of the MWCNT (higher hardness values). Raman spectroscopy (Horiba HR800 equipment, a laser incident beam with a 442 nm wavelength) was used to evaluate the effect of the best processing condition (resulting with the maximum hardness value for Al-MWCNT) on the integrity of MWCNTs. Afterwards, the best composition and dispersing condition were selected for mixing other reinforcements (graphene, nanoalumina, and WC) with the Al powder in an equal vol. %. The solid concentrations (g/mL) of these reinforcements in the isopropanol was similar to that of the nanotubes except for the WC particles which was almost 4 times greater than the other reinforcements, due to the preparation limitations. The dispersion evaluation was carried out by the SEM and TEM; EBSD was used for the determination of the crystallographic orientation of the grains of the reinforced specimens.

3. Results

3.1. Preliminary Preparation of the Alyminium Multi-Walled Carbon Naotube (Al-MWCNT)

Microscopy observations highlight the dispersion of the nanotubes before compaction and sintering. It will be noted that the MWCNT agglomerates surrounded fine and large particles (Figure 2a,b) and that some short ones are apparently placed on individual Al particles (Figure 2c).

Microhardness measurements of the preliminary Al-MWCNT nanocomposites (Table 2) showed that the Al-0.5 wt. % MWCNT became the hardest, in respect to the non-reinforced matrix. Microscopy observations of the preliminary sintered specimens revealed that the more the MWCNT concentration was used, the larger were the MWCNT agglomerates observed. They also revealed some nanotubes joining two separated zones in a fracture in the Al matrix, which shows the CNT bridging effect (Figure 2d), it will be discussed in Section 4.

Table 2. Microhardness values of specimens compacted at ~300 MPa and sintered.

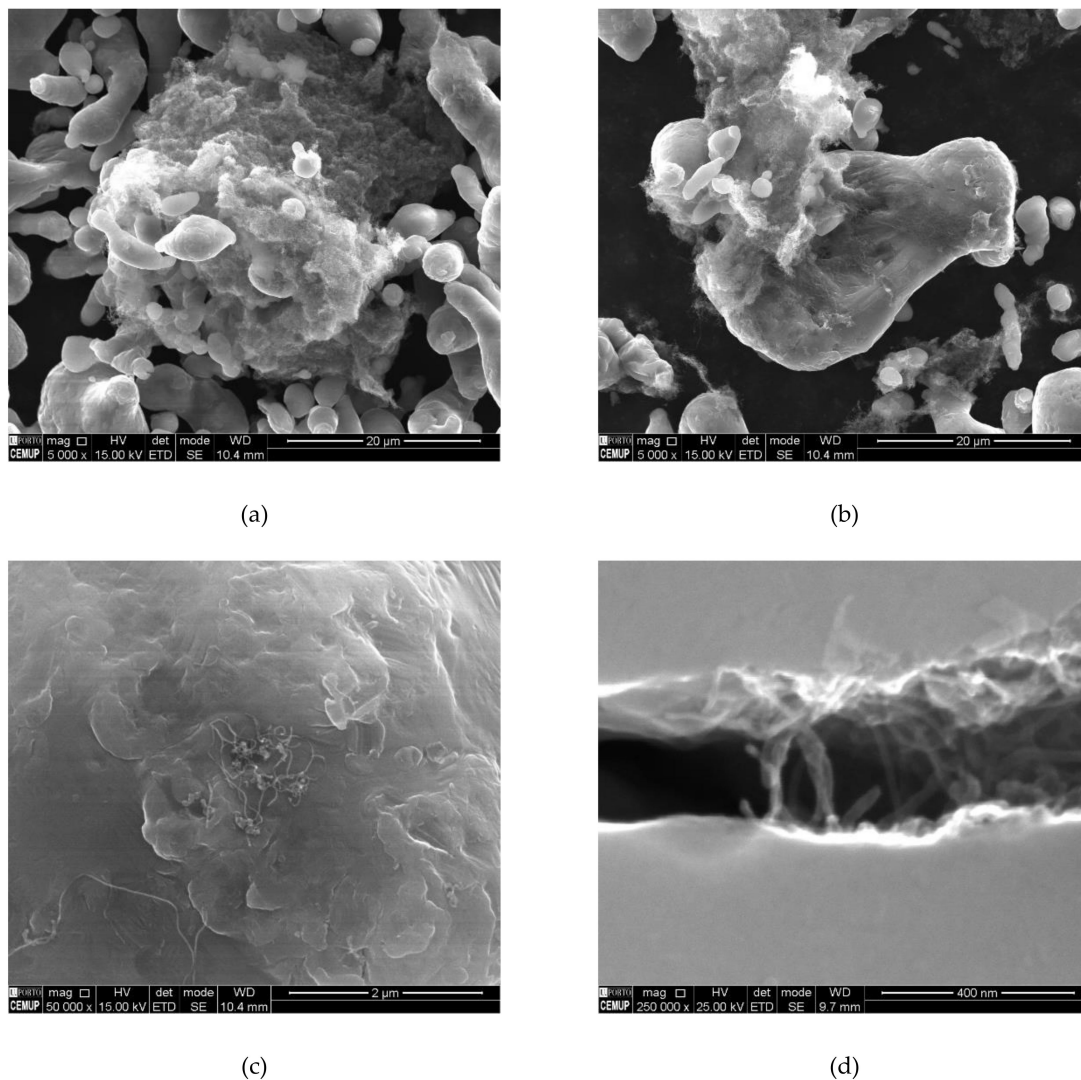| MWCNT (wt. %)	0.00	0.25	0.50	0.75	1.00	2.00
HV 0.01	35	38	40	38	39	39
SD	3	2	2	3	3	3

(a)

(b)

(c)

(d)

Figure 2. SEM/SE images of Al-0.75 wt. % MWCNT: (**a**), (**b**), and (**c**) dispersion of the constituents before compaction; and (**d**) cross section of the sintered specimen at the end of a prolonged crack in a hardness indentation point.

3.2. Changing the Dispersing Conditions for the Al-MWCNT System

In order to surpass the hardness measured in the preliminary results (Table 2), the dispersing conditions of the MWCNT were changed. While it did not correspond to the composition that led to the greatest hardness, the 0.75 wt. % MWCNT composition was selected for new dispersing conditions to establish a comparison with related studies [24,25]. New changes involved the speed and time of mixing, the order of adding constituents into isopropanol, using Stearic Acid (SA) and Hydrogen Peroxide (H_2O_2) as surfactants, and increasing the compaction level (from 300 MPa to 400 MPa) to eliminate possible green porosities (Table 3). It will be seen that the hardness of the pure Al and of the reinforced specimen increased slightly (comparing the specimens Nos. 1 and 2 in Table 3 with corresponding specimens in Table 2), as the compaction pressure had increased. Meanwhile, no hardness increase was observed when the mixture quantity in the mixing dish had increased (comparing specimens Nos. 2 and 3 in Table 3). This condition was carried out for large scale processing, and the SEM evaluation hardly revealed any MWCNT placed on the individual Al particles. Applying post mixing treatment, such as Turbula over a long period, or even changing the order of mixing (No. 4 to No. 8 in Table 3), did not increase the hardening effect. Adding SA to

isopropanol or using H_2O-5 vol. % H_2O_2 as the dispersing solution was not helpful either (No. 9 and No. 10 in Table 3).

Table 3. Microhardness values specimens, 0.75 wt. % MWCNT, compacted at ~400 MPa and sintered.

No.	Conditions	HV 0.01	SD
1	Pure Al	36	1
2	Sonicated like preliminary condition	39	3
3	Sonicated like preliminary condition but in an amount approximately 10 times greater in the mixing dish	37	5
4	Sonicated like preliminary condition and then 24 h in Turbula	39	3
5	MWCNTs and Al sonicated 5 min separately and then 10 min together	36	4
6	Like No. 5 and then 6 h in Turbula	37	3
7	Sonicated like preliminary condition and then magnetic stirring	36	3
8	MWCNTs and Al sonicated 10 min separately and then 5 min together followed by magnetic stirring	39	6
9	Sonicated like preliminary condition with 5 wt. % SA	36	3
10	Sonicated like preliminary condition in H_2O-5 vol. % H_2O_2	37	2

3.3. Application of Ultrasonication Bath to Assist Sonication

Since the MWCNT agglomerations affect the matrix strengthening [31], the ultrasonication technique was applied to facilitate the MWCNT separation. An isopropanol-MWCNT mixture with a very small concentration (~1.5×10^{-4} g/mL) of MWCNT was placed in the ultrasonication bath for 60 min, and specimens were taken for microscopy observations after 0, 15, and 60 min of dispersion. The analysis of Figures 1b and 3a–d shows that the longer the ultrasonication time, the smaller the agglomerates. Microscopy observations also highlighted the fact that the MWCNTs, after being processed for 60 min, were not exfoliated even when they were processed by the high speed sonication for 15 min (Figure 3e).

The ultrasonication bath itself was not able to disperse the Al powder particles with MWCNTs completely, and some Al was always deposited on the bottom of the dispersing dish. To ensure a complete dispersion a new approach, the "assisted sonication", was tested in such a way that firstly the ultrasonication bath was applied to disperse the MWCNTs in isopropanol, and secondly the Al powder was added and the dispersion proceeded by applying the sonication and ultrasonication simultaneously. This application was not effective in increasing the hardness for the ultimate and medium speed stirring conditions (Nos. 1 and 2 in Table 4). It can be seen that when the dispersing speed of the final mixing step decreased, the microhardness increased slightly (No. 3 in Table 4). It improved a little when the primary dispersing time decreased, and the dispersing speed for the second step increased (No. 4 in Table 4).
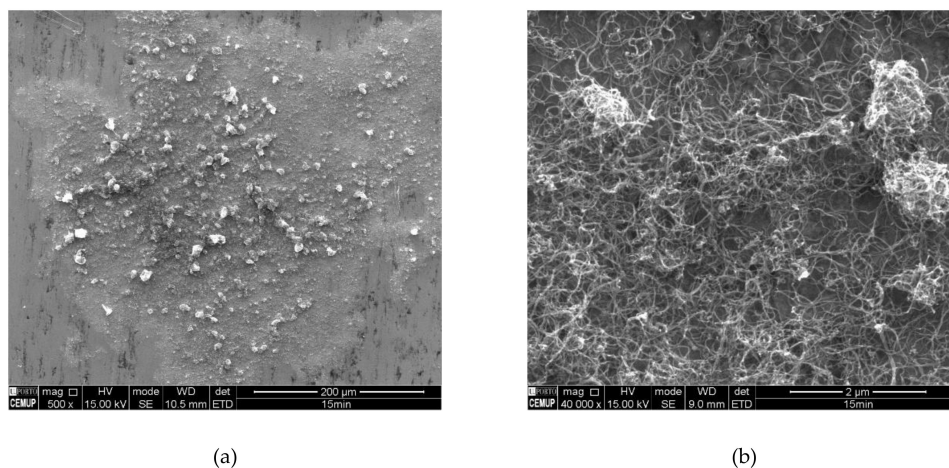

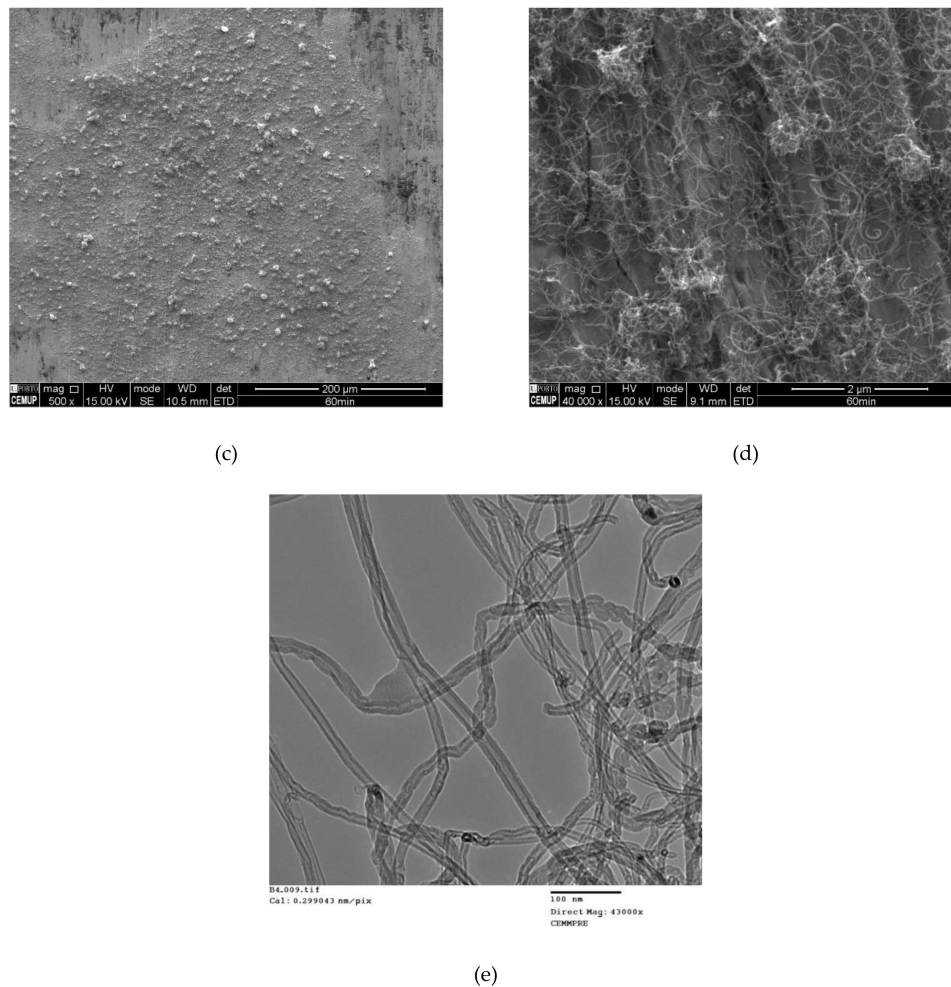(a)   (b)

Figure 3. *Cont.*

(c)

(d)

(e)

Figure 3. SEM/SE images from ~1.7 g/mL MWCNT in isopropanol solution treated in an ultrasonication bath (35 kHz) after (**a**) and (**b**) 15 min, and (**c**) and (**d**) 60 min; (**e**) TEM image from the nanotubes processed by the assisted sonication method (60 min' ultrasonication followed by a simultaneous sonication for 15 min at 20,400 rpm).

Table 4. Microhardness of Al-0.75 wt. % MWCNT prepared by the assisted sonication method, compacted at ~400 MPa and sintered.

No.	Conditions	HV 0.01	SD
1	MWCNT in Ultrasonic bath for 60 min, 3000 rpm Al 5 min, and then 20,400 rpm together for 15 min cooperated by ultrasonication	36	2
2	MWCNT in Ultrasonic bath for 60 min, 3000 rpm Al 5 min, and then 11,000 rpm together for 15 min cooperated by ultrasonication	36	3
3	MWCNT in Ultrasonic bath for 60 min, 3000 rpm Al 5 min, and then 1,500 rpm together for 15 min cooperated by ultrasonication	38	2
4	MWCNT in Ultrasonic bath for 15 min, 3000 rpm Al 5 min, and then 11,000 rpm together for 5 min cooperated by ultrasonication	41	2

3.4. Al Powder Mixed with Graphene, Alumina and WC

The optimized sonication assisted method, i.e., ultrasonic bath for 15 min, 3,000 rpm Al 5 min, and then 11,000 rpm together for 5 min cooperated by ultrasonication (No. 4 in Table 4) was selected to disperse graphene, nanoalumina, and ultrafine WC with Al powder, in individual batches. According to the densities of the Al and MWCNT, the 0.75 wt. % MWCNT mixture corresponded to 1 vol. % MWCNT. This volume fraction was also selected to prepare the nanocomposites reinforced with graphene, nanoalumina, and ultrafine WC. The microhardness results (Table 5) showed that

the Al-WC system was strengthened the most, while graphene and nanoalumina achieved the same level of hardness. As regards the density, graphene nanocomposites showed the highest densification, followed by WC and nanoalumina.

Table 5. Microhardness and densification of Al mixed with 1 vol. % of the nano/ultrafine reinforcements by means of the assisted sonication method, pressed (152 MPa) and sintered.

Material	Pure	MWCNT	Graphene	Alumina	WC
HV 0.01	30 ± 1	31 ± 2	36 ± 1	36 ± 1	46 ± 2
Densification (%)	99 ± 2	95 ± 0	99 ± 1	96 ± 0	97 ± 1

3.5. Raman Analysis of MWCNT

Raman spectroscopy was used to evaluate the effect of the assisted sonication technique on the MWCNTs, and whether the nanotubes were affected by the presence of the Al powder during dispersion. This was carried out by testing three specimens: the pristine MWCNT, the nanotube processed by means of the assisted sonication, and the Al-1 vol. % MWCNT dispersed by the same technique (Figure 4). The changes of intensity ratios of the three specimens, I_D/I_G, show a slight reduction for the sonication assisted MWCNT, and an increase for the Al-1 vol. % MWCNT mixture (Table 6). It was also observed that the frequency of the D band, disorder-induced feature, decreased with the sonication but remained the same for the powder mixture. The frequency of the G band, representing the tangential vibration, was upshifted after each experiment.

Table 6. The positions of D and G bands, and the I_D/I_G.

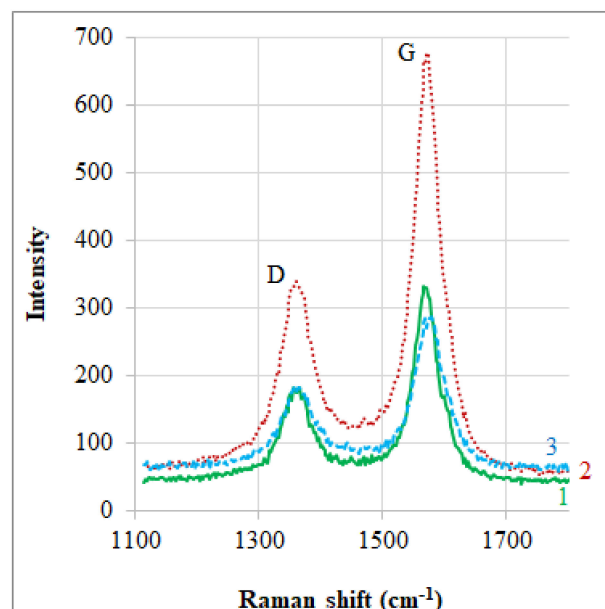| Specimen	D (cm^{-1})	G (cm^{-1})	I_D/I_G
Pristine	1365.5	1566.9	0.55
Sonication assisted	1358.3	1571.6	0.50
Sonication assisted with powder	1358.3	1578.7	0.64

Figure 4. Raman spectra taken, first order region, from pristine MWCNT (No. 1 in green), assisted sonication MWCNT (No. 2 in red), and assisted sonication Al-1 vol. % MWCNT (No. 3 in blue).

4. Discussions

Comparing the preliminary results (Table 2) with the related study, the same preparation conditions and the same MWCNT [24] having been applied, we see that the metallic particle characteristics (4S) influenced the strengthening, i.e., 14% hardness increase by 0.5 wt. % MWCNT, unlike the related study in which the increase of 47% was reported by 0.75 wt. % MWCNT, this reinforcement was associated with a good dispersion of the nanotubes in the Al matrix and the Al/CNT interface as well.

Related studies reported the bridging effect at the fracture surface of the reinforced specimens [23,32–34]; a similar effect was observed in this study (Figure 2a), although the associated strengthening was not very strong. Microscopy observations highlighted that the crack, nucleated in a hardness indentation, had propagated through the MWCNT agglomerates to a region of the matrix where the nanotubes made it difficult to sinter the aluminum particles. This heterogeneous region indicates the presence of a weak interface, CNT/matrix, the load transfer mechanism having been weakened [31].

Sonication is a physical dispersion method through which high energy stirring causes strong shear forces in the solution. Due to this, bubbles form and break down the MWCNT agglomerates [35]. However, there were still large MWCNT agglomerates, bigger than the Al particles, after sonication at 20,400 rpm for 15 min (Figure 2b–d). Therefore, these results could indicate that the new Al powder (with different 4S—Table 1) did not contribute efficiently to breaking down the MWCNT agglomerates. This efficiency was also affected by the mixture quantity in the dispersing dish, i.e., when this quantity increased by almost ten times, the hardness decreased slightly (Nos. 2 and 3 in Table 3). This absence of strengthening is attributed to the reduction in dispersing efficiency, which was confirmed by the SEM observations, i.e., no MWCNT was found on individual Al particles, as was observed in Figure 2d.

It was reported that increasing the sonication time, for dispersing, was not advantageous because MWCNTs were damaged due to the introduction of higher energies [25]. This is an important finding, since defects in MWCNTs are prone to form aluminum carbide [36–38]; therefore the ultrasonication mixing method was opted for. The microscopy observations (Figure 3a–d) revealed that the size of MWCNT aggregates was reduced when the ultrasonication time increased to 60 min at 35 kHz. It is noted that the formation of shock waves, due to bubbles collapsing as a result of the ultrasonication technique [39], is not as aggressive as the shear bubbles, generated by sonication. TEM observations confirmed that the MWCNTs were not exfoliated after the assisted sonication process (Figure 3e).

Applying common sonication and the assisted sonication techniques resulted in a hardness increase of 8% (No. 2 in Table 3) and 14% (No. 4 in Table 4). This improvement is attributed to the dispersion of the MWCNTs; as seen in Figure 5a,b, the size and dispersion of agglomerates changed (a maximum size of ~75 μm decreased to ~20 μm), although some porosities may have been associated with this. This hardness increase is still a long way from what should be expected and indicates, as above mentioned, that the 4S of the powder should play an important role in the strengthening. Moreover, the compaction level (a reduction of 400 MPa to 152 MPa, Tables 3 and 4) had a great influence on the hardness which is attributed to the densification of the nanocomposite (No. 1 in Table 3 and No. 4 in Table 4 compared with Table 5).

As regards the integrity of MWCNTs after applying the assisted sonication method, the MWCNT agglomerates were broken through bubble collapsing, whereby the nanotubes were forced to face a certain level of strain during the process. The Raman analysis revealed the consequences of this effect, i.e., an association of bands shifting over the entire process, and this was pronounced for the G band in the presence of the Al powder. Band shifting due to the strain has already been mentioned in related studies [38,40,41]. Moreover, the I_D/I_G ratio, as a criterion for determining the disorder level [30], decreased for the MWCNTs in the absence of powder (Table 6), and the G band upshifted a little. This could mean that the assisted sonication method has acted as a sort of cleaning process, i.e., the interlocked impurities can be eliminated, thereby facilitating the tangential vibration. It was observed that the intensity ratio increased when the nanotubes were processed in the presence of the Al powder. Therefore, some level of defects should have been introduced into the MWCNT structure,

which would accord with other authors [38]. However, it seems that the assisted sonication method is much less aggressive to MWCNTs than ball milling [41], and if this ratio is slightly greater than that of the ratio reported in the related study [24], this can be attributed to the associated effect of the powder characteristics (different 4S).
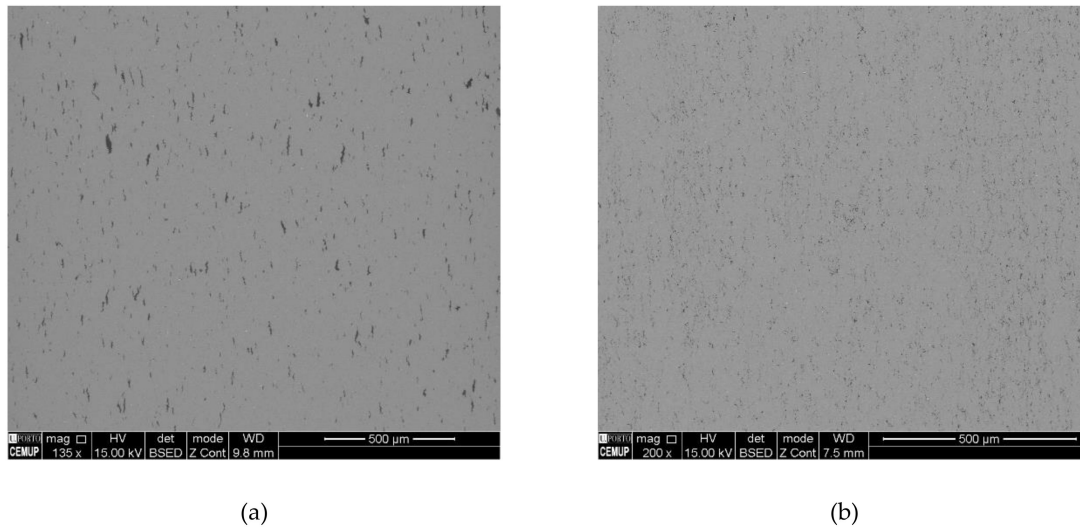

(a)   (b)

Figure 5. SEM/BSE image from 0.75 wt. % MWCNT composite after (**a**) normal sonication method, as described in No. 2 in Table 3; and (**b**) assisted sonication method, as seen in No. 4 in Table 4.

Application of the assisted sonication method for the graphene nanocomposite led to a higher hardening effect than that of the MWCNT (20% as compared with 14%), although no significant difference was observed between the distribution of the constituents (Figures 5b and 6a). Detailed observations revealed that multilayer graphene sheets still existed after ultrasonication (Figure 6b), even after applying the assisted sonication process with Al powder. However, high-resolution TEM is needed for further precise analysis, e.g., to reveal whether the nano sheets were damaged. This increase in hardness can be attributed to the graphene rigidity itself and the grain size refinement (7.0 ± 3.6 μm for the Pure Al to 5.7 ± 3.1 μm for the Al-Graphene, analyzed by SEM/EBSD). Qualitative observations indicated that the graphene and the processing conditions did not introduce any preferential crystallographic orientation because no color was predominant (Figure 7). Related studies reported a growth in hardness of ~15% for Al composite mixed with 1 wt. % graphene nanosheets, produced by four h of dispersing through ultrasonication followed by spark plasma sintering at 400 °C in a vacuum with the application of a uniaxial pressure of 50 MPa [20]. Some authors reported a growth of 43% in hardness for the Al composite, mixed with 0.15 wt. % exfoliated graphene nanosheets. The preparation involved 48 h dispersal by magnetic stirring of the as-prepared graphene with Al powder, compacting at 560 MPa and sintering at 600 °C for 4 h in an Argon atmosphere [42]. The difference between these reports and the results of this study (graphene nanocomposite in Table 5) can be attributed to the dispersion methods, characteristics of the Al powder, type and volume fraction of the graphene, and the thermomechanical history of the nanocomposites.
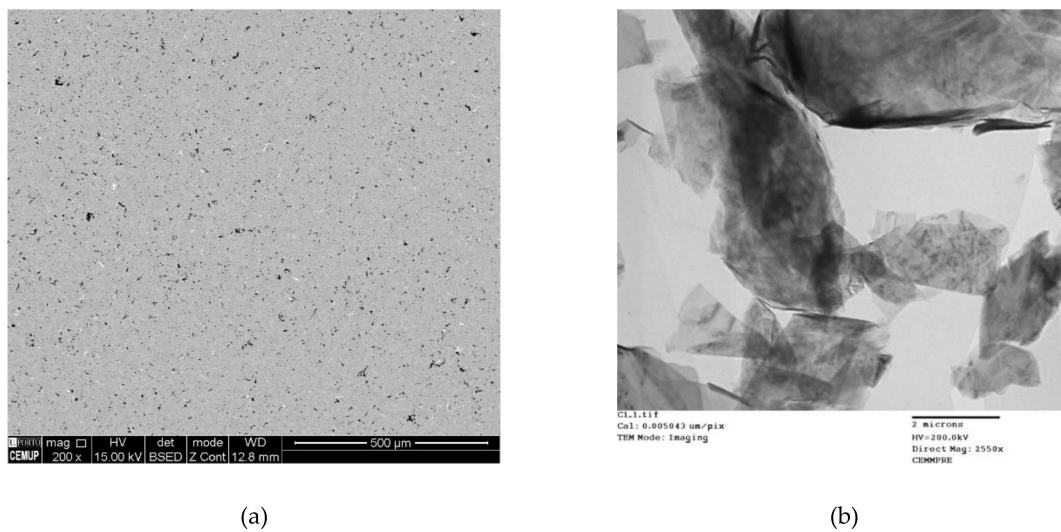
Figure 6. (**a**) SEM/BSE image from the as polished surface of the sintered Al-1 vol. % Graphene specimen; (**b**) TEM image showing the presence of graphene multi sheets after 15 min' ultrasonication.
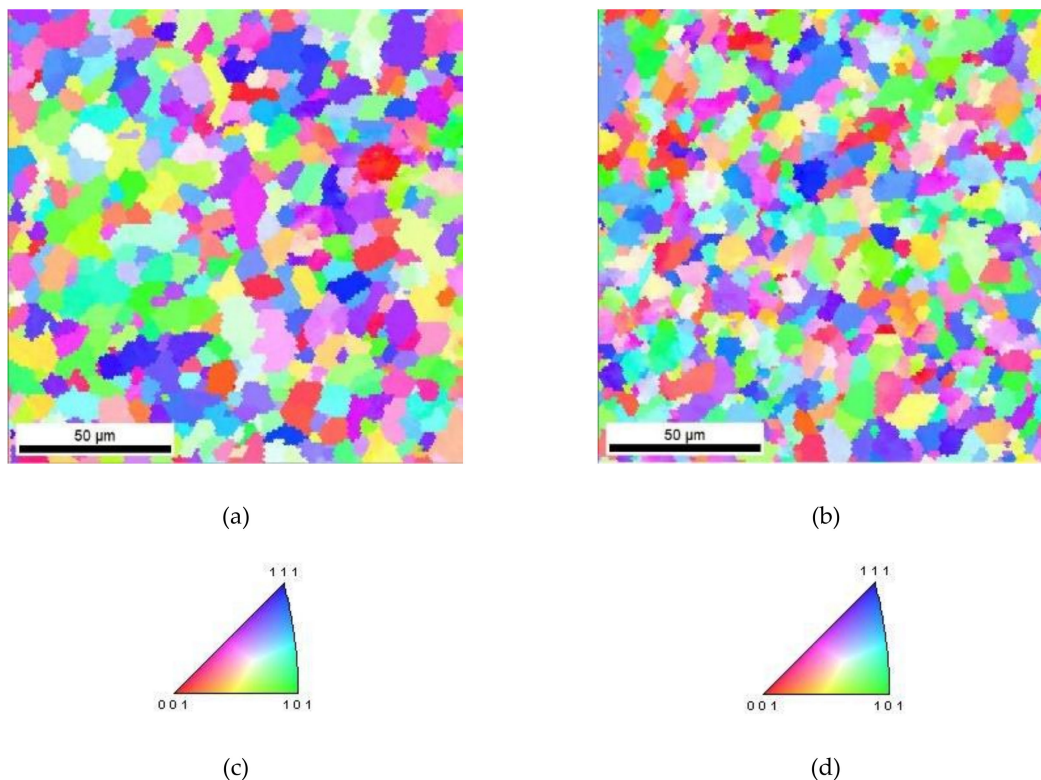

Figure 7. The inverse pole figures (IPF) of the (**a**) pure Al and (**b**) Al-Graphene, and their corresponding coded maps, respectively, (**c**) and (**d**) (SEM/EBSD).

With regard to the Al-Al$_2$O$_3$ nanocomposite, although this resulted in a hardness value similar to the Al-Graphene composite, it presented a lower densification than the pure Al (Table 5). This reduction can be explained by the dispersion of the nanoalumina particles among the Al powder (Figure 8); they are seen in agglomerates as big as Al particles, and also in very fine distributions on the Al particle surfaces, i.e., they could behave as a barrier against the volume diffusion of aluminium during sintering. A related study [43] reported a hardness growth of 109% for an Al reinforced by 4 vol. % Al$_2$O$_3$. This large difference in strengthening cannot be related only to the volumetric portion of

the reinforcement, but also to the processing conditions (combination of wet mixing, cold isostatic pressing, sintering proceeded by hot extrusion and annealing).
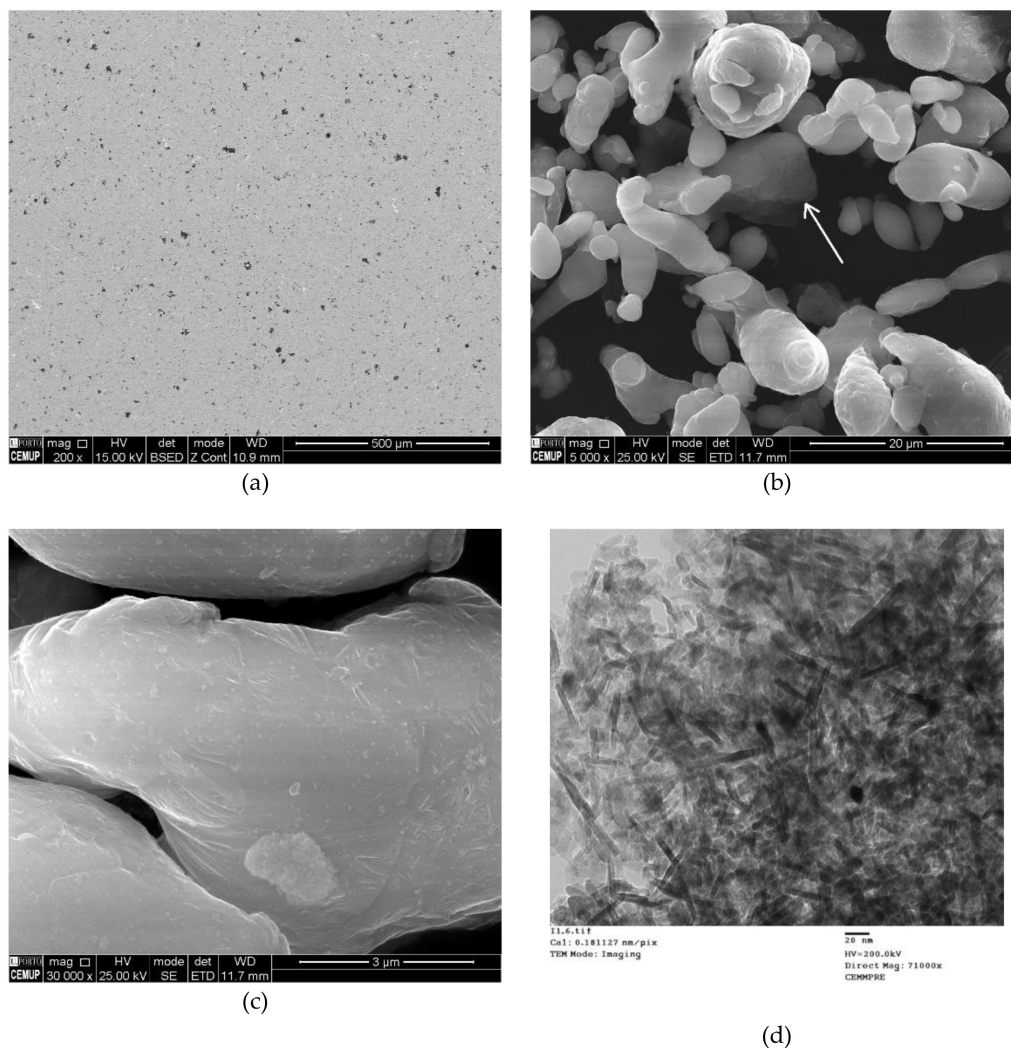

Figure 8. SEM/SE images showing (**a**) the as polished surface of the sintered Al-1 vol. % Nanoalumina specimen; (**b**) the presence of large agglomerates among Al particles (white arrow); and (**c**) fine distributions on particle surfaces; and (**d**) TEM image from nanoalumina agglomerate after ultrasonication for 15 min.

According to microhardness measurements (Table 5), the Al matrix attained a hardness increase of 53% by means of ultrafine WC. The grain size analysis, conducted using the SEM/EBSD technique, indicated a grain size refinement from 7.0 ± 3.6 µm, for the pure Al, to 4.3 ± 2.7 µm, for the Al-WC composite, thus the contribution of Hall-Petch mechanism can be considered. Meanwhile, no preferential crystallography orientation was confirmed in the Al matrix (Figure 9a). The microstructure of the Al-WC composite comprises the Al matrix with a new greyish phase, larger than the primary WC particle size, and non-reacted WC particles (Figure 9b). The phase formed is indicated as $Al_{12}W$, according to stoichiometry obtained by electron dispersive spectroscopy analysis, and it is consistent with other studies [44,45]. Thus, the hardening effect in Al-WC can be caused by three occurrences: The grain size refinement, phase transformation, and the non-reacted dispersed WC particles. Hence, the assisted sonication method has been able to disperse WC particles that are much heavier than the Al particles, although the reinforcement concentration in the dispersion solution was almost four times higher than that of the other reinforcements used in this study. Microscopy analyses also reveal that the $Al_{12}W$ phase can contribute to the reduction of densification

in respect to the pure Al. Related studies reported the strengthening effect of the WC in the Al matrix through other PM approaches, e.g., ball milling, it being reported that the hardness increases with the increase in both the milling time and the WC content [44]; ~23% increase in the hardness obtained by 15 wt. % WC, with a reverse effectiveness caused by increasing the milling time [45]; a hardness increase of 40% by 10 wt. % WC [46]; or an incremental hardness growth resulting from increasing the amount of WC with an opposite effect on tensile strength and densification [47]. It is seen that all these high hardness increases were obtained by adding large amounts of WC through which the density is affected considerably, while the hardening effect in this study was obtained by 1 vol. %.

(a)

(b)

(c)

(d)

Figure 9. (**a**) and (**b**) SEM/EBSD analysis illustrating the IPF and coded map of the Al matrix; (**c**) SEM/BSE images illustrating the WC and the phase formed after sintering; and (**d**) distribution of WC in Al powder.

5. Conclusions

In this study, aluminum powders, with D_{50} of 10 μm, were mixed with carbon nanotubes, graphene nanosheets, nanoalumina, and ultrafine tungsten carbide.

Mechanical characterization of Al–MWCNT nanocomposites reveals a weak hardening effect with the maximum hardness obtained for 0.5 wt. % MWCNT after sonication and sintering. Comparison with other studies indicates a strong influence of the aluminum powder characteristics (surface area, size distribution, shape factor and structure-4S) in the mechanical response of the nanocomposite.

This study shows that sonication assisted by an ultrasonication bath is the most appropriate method for dispersing MWCNTs without causing damage. This dispersal method has been effective for dispersing the other reinforcements.

Under the same processing conditions and with similar volume percentages, the greatest hardening effect was achieved by using the ultrafine WC particles coming after by graphene nanosheets, nanoalumina, and MWCNT. This was obtained by a good dispersion of dense WC in Al powder through the assisted sonication method. The strengthening can be a combination of phase formation, grain refinement, and fine WC particle dispersion.

References

1. Zhou, D.S.; Qiu, F.; Wang, H.Y.; Jiang, Q.C. Manufacture of nano-sized particle-reinforced metal matrix composites: A review. *Acta Metall. Sin. Engl. Lett.* **2014**, *27*, 798–805. [CrossRef]
2. Bakshi, S.R.; Lahiri, D.; Agarwal, A. Carbon nanotube reinforced metal matrix composites-a review. *Inter. Mater. Rev.* **2010**, *55*, 41–64. [CrossRef]
3. Baig, Z.; Mamat, O.; Mustapha, M. Recent progress on the dispersion and the strengthening effect of carbon nanotubes and graphene-reinforced metal nanocomposites: A review. *Crit. Rev. Solid State Mater. Sci.* **2018**, *43*, 1–46. [CrossRef]
4. Deng, C.F.; Wang, D.Z.; Zhang, X.X.; Li, A.B. Processing and properties of carbon nanotubes reinforced aluminum composites. *Mater. Sci. Eng. Struct. Mater. Prop. Microstruct. Process.* **2007**, *444*, 138–145. [CrossRef]
5. Bisht, A.; Srivastava, M.; Kumar, R.M.; Lahiri, I.; Lahiri, D. Strengthening mechanism in graphene nanoplatelets reinforced aluminum composite fabricated through spark plasma sintering. *Mater. Sci. Eng. Struct. Mater. Prop. Microstruct. Process.* **2017**, *695*, 20–28. [CrossRef]
6. Vaisman, L.; Wagner, H.D.; Marom, G. The role of surfactants in dispersion of carbon nanotubes. *Adv. Colloid Interface Sci.* **2006**, *128*, 37–46. [CrossRef] [PubMed]
7. Ashby, M.F.; Ferreira, P.J.; Schodek, D.L. Nanomaterials: Properties. In *Nanomaterials, Nanotechnologies and Design*; Butterworth-Heinemann: Boston, MA, USA, 2009; pp. 199–255.
8. Spowart, J.E.; Miracle, D.B. The influence of reinforcement morphology on the tensile response of 6061/SiC/25p discontinuously-reinforced aluminum. *Mater. Sci. Eng. Struct. Mater. Prop. Microstruct. Process.* **2003**, *357*, 111–123. [CrossRef]
9. Tjong, S.C. Novel nanoparticle-reinforced metal matrix composites with enhanced mechanical properties. *Adv. Eng. Mater.* **2007**, *9*, 639–652. [CrossRef]
10. Akbari, M.K.; Baharvandi, H.R.; Shirvanimoghaddam, K. Tensile and fracture behavior of nano/micro TiB$_2$ particle reinforced casting A356 aluminum alloy composites. *Mater. Des.* **2015**, *66*, 150–161. [CrossRef]
11. Casati, R.; Vedani, M. Metal matrix composites reinforced by nano-particles—A review. *Metals* **2014**, *4*, 65–83. [CrossRef]
12. Lumley, R. *Fundamentals of Aluminium Metallurgy Production, Processing and Applications*; Woodhead Publishing Limited: Cambridge, UK, 2011; p. 7.
13. Williams, J.C.; Starke, E.A. Progress in structural materials for aerospace systems. *Acta Mater.* **2003**, *51*, 5775–5799. [CrossRef]
14. Koli, D.K.; Agnihotri, G.; Purohit, R. Advanced aluminium matrix composites: The critical need of automotive and aerospace engineering fields. *Mater. Today Proc.* **2015**, *2*, 3032–3041. [CrossRef]

15. He, F. Ceramic nanoparticles in metal matrix composites. In *Ceramic Nanocomposites*; Woodhead Publishing: Cambridge, UK, 2013; pp. 185–207.

16. Cintas, J.; Cuevas, F.G.; Montes, J.M.; Caballero, E.S.; Herrera, E.J. Strengthening of ultrafine PM aluminium using nano-sized oxycarbonitride dispersoids. *Mater. Sci. Eng. Struct. Mater. Prop. Microstruct. Process.* **2011**, *528*, 8286–8291. [CrossRef]

17. Esawi, A.M.K.; Morsi, K.; Sayed, A.; Taher, M.; Lanka, S. The influence of carbon nanotube (CNT) morphology and diameter on the processing and properties of CNT-reinforced aluminium composites. *Compos. Part Appl. Sci. Manuf.* **2011**, *42*, 234–243. [CrossRef]

18. Hu, Z.; Tong, G.; Lin, D.; Chen, C.; Guo, H.; Xu, J.; Zhou, L. Graphene-reinforced metal matrix nanocomposites—A review. *Mater. Sci. Technol.* **2016**, *32*, 930–953. [CrossRef]

19. Nieto, A.; Bisht, A.; Lahiri, D.; Zhang, C.; Agarwal, A. Graphene reinforced metal and ceramic matrix composites: A review. *Int. Mater. Rev.* **2017**, *62*, 241–302. [CrossRef]

20. Tian, W.M.; Li, S.M.; Wang, B.; Chen, X.; Liu, J.H.; Yu, M. Graphene-reinforced aluminum matrix composites prepared by spark plasma sintering. *Int. J. Miner. Metall. Mater.* **2016**, *23*, 723–729. [CrossRef]

21. Noguchi, T.; Magario, A.; Fukazawa, S.; Shimizu, S.; Beppu, J.; Seki, M. Carbon nanotube/aluminium composites with uniform dispersion. *Mater. Trans.* **2004**, *45*, 602–604. [CrossRef]

22. Liao, J.Z.; Tan, M.J. Mixing of carbon nanotubes (CNTs) and aluminum powder for powder metallurgy use. *Powder Technol.* **2011**, *208*, 42–48. [CrossRef]

23. Kwon, H.; Estili, M.; Takagi, K.; Miyazaki, T.; Kawasaki, A. Combination of hot extrusion and spark plasma sintering for producing carbon nanotube reinforced aluminum matrix composites. *Carbon* **2009**, *47*, 570–577. [CrossRef]

24. Simões, S.; Viana, F.; Reis, M.A.L.; Vieira, M.F. Improved dispersion of carbon nanotubes in aluminum nanocomposites. *Compos. Struct.* **2014**, *108*, 992–1000. [CrossRef]

25. Simões, S.; Viana, F.; Reis, M.A.L.; Vieira, M.F. Influence of dispersion/mixture time on mechanical properties of Al–CNTs nanocomposites. *Compos. Struct.* **2015**, *126*, 114–122. [CrossRef]

26. Chen, Z.K.; Yang, J.P.; Ni, Q.Q.; Fu, S.Y.; Huang, Y.G. Reinforcement of epoxy resins with multi-walled carbon nanotubes for enhancing cryogenic mechanical properties. *Polymer* **2009**, *50*, 4753–4759. [CrossRef]

27. Li, Y.; Chen, C.X.; Zhang, S.; Ni, Y.W.; Huang, J. Electrical conductivity and electromagnetic interference shielding characteristics of multiwalled carbon nanotube filled polyacrylate composite films. *Appl. Surf. Sci.* **2008**, *254*, 5766–5771. [CrossRef]

28. Ciesielski, A.; Samori, P. Graphene via sonication assisted liquid-phase exfoliation. *Chem. Soc. Rev.* **2014**, *43*, 381–398. [CrossRef] [PubMed]

29. Simões, S.; Viana, F.; Reis, M.A.L.; Vieira, M.F. Aluminum and nickel matrix composites reinforced by CNTs: Dispersion/Mixture by ultrasonication. *Metals* **2017**, *7*, 279. [CrossRef]

30. Costa, S.; Borowiak-Palen, E.; Kruszynska, M.; Bachmatiuk, A.; Kalenczuk, R.J. Characterization of carbon nanotubes by Raman spectroscopy. *Mater. Sci. Pol.* **2008**, *26*, 433–441.

31. Barai, P.; Weng, G.J. A theory of plasticity for carbon nanotube reinforced composites. *Int. J. Plast.* **2011**, *27*, 539–559. [CrossRef]

32. Rikhtegar, F.; Shabestari, S.G.; Saghafian, H. Microstructural evaluation and mechanical properties of Al–CNT nanocomposites produced by different processing methods. *J. Alloys Compd.* **2017**, *723*, 633–641. [CrossRef]

33. Boesl, B.; Lahiri, D.; Behdad, S.; Agarwal, A. Direct observation of carbon nanotube induced strengthening in aluminum composite via in situ tensile tests. *Carbon* **2014**, *69*, 79–85. [CrossRef]

34. Xia, Z.; Riester, L.; Curtin, W.A.; Li, H.; Sheldon, B.W.; Liang, J.; Chang, B.; Xu, J.M. Direct observation of toughening mechanisms in carbon nanotube ceramic matrix composites. *Acta Mater.* **2004**, *52*, 931–944. [CrossRef]

35. Cheng, Q.H.; Debnath, S.; Gregan, E.; Byrne, H.J. Ultrasound-assisted SWNTs dispersion: Effects of sonication parameters and solvent properties. *J. Phys. Chem. C* **2010**, *114*, 8821–8827. [CrossRef]

36. Ci, L.J.; Ryu, Z.Y.; Jin-Phillipp, N.Y.; Ruhle, M. Investigation of the interfacial reaction between multi-walled carbon nanotubes and aluminum. *Acta Mater.* **2006**, *54*, 5367–5375. [CrossRef]

37. Bustamante, R.P.; Yoshida, M.M.; Sánchez, R.M.; Martinez, J.B.; Cantu, J.G. Al4C3 Formation in carbon nanotube/Aluminum composites. *Microsc. Microanal.* **2012**, *18*, 1914. [CrossRef]

38. Poirier, D.; Gauvin, R.; Drew, R.A.L. Structural characterization of a mechanically milled carbon nanotube/aluminum mixture. *Compos. Part A Appl. Sci. Manuf.* **2009**, *40*, 1482–1489. [CrossRef]

39.   Huang, Y.Y.; Terentjev, E.M. Dispersion of carbon nanotubes: Mixing, sonication, stabilization, and composite properties. *Polymers* **2012**, *4*, 275–295. [CrossRef]

40.   Reis, M.A.L.; Neto, N.M.B.; de Sousa, M.E.S.; Araujo, P.T.; Simoes, S.; Vieira, M.F.; Viana, F.; Loayza, C.R.L.; Borges, D.J.A.; Cardoso, D.C.S.; et al. Raman spectroscopy fingerprint of stainless steel-MWCNTs nanocomposite processed by ball-milling. *Aip Adv.* **2018**, *8*, 015323. [CrossRef]

41.   Ostovan, F.; Matori, K.A.; Toozandehjani, M.; Oskoueian, A.; Yusoff, H.M.; Yunus, R.; Ariff, A.H.M. Nanomechanical behavior of multi-walled carbon nanotubes particulate reinforced Aluminum nanocomposites prepared by Ball Milling. *Materials* **2016**, *9*, 140. [CrossRef] [PubMed]

42.   Liu, J.H.; Khan, U.; Coleman, J.; Fernandez, B.; Rodriguez, P.; Naher, S.; Brabazon, D. Graphene oxide and graphene nanosheet reinforced aluminium matrix composites: Powder synthesis and prepared composite characteristics. *Mater. Des.* **2016**, *94*, 87–94. [CrossRef]

43.   Kang, Y.C.; Chan, S.L.I. Tensile properties of nanometric Al_2O_3 particulate-reinforced aluminum matrix composites. *Mater. Chem. Phys.* **2004**, *85*, 438–443. [CrossRef]

44.   Evirgen, A.; Ovecoglu, M.L. Characterization investigations of a mechanically alloyed and sintered Al-2 wt. %Cu alloy reinforced with WC particles. *J. Alloys Compd.* **2010**, *496*, 212–217. [CrossRef]

45.   Simon, A.; Lipusz, D.; Baumli, P.; Balint, P.; Kaptay, G.; Gergely, G.; Sfikas, A.; Lekatou, A.; Karantzalis, A.; Gacsi, Z. Microstructure and mechanical properties of Al-WC composites. *Arch. Metall. Mater.* **2015**, *60*, 1517–1521. [CrossRef]

46.   Fabian, S.J.A.; Selvam, B. Experimental investigation of densification and mechanical behaviour on Aluminum reinforced with WCp metal matrix composite prepared by powder metallurgy. *J. Mech. Eng. Technol.* **2014**, *6*, 1–11.

47.   Razavi, M.; Mobasherpour, I. Production of aluminum nano-composite reinforced by tungsten carbide particles via mechanical milling and subsequent hot pressing. *Int. J. Mater. Res.* **2014**, *105*, 1103–1110. [CrossRef]